Research Square

Preprints are preliminary reports that have not undergone peer review.
They should not be considered conclusive, used to inform clinical practice,
or referenced by the media as validated information.

Inhibition of both Anoctamin 1 and Transient Receptor Potential Vanilloid 4 Channels is critical for attenuation of perspiration

Moe Iwata
Nagoya City University
Katsuki Kitai
IKEDA MOHANDO CO.,LTD
Kenji Sano
Kanazawa Medical University
Hitoshi Kawada
IKEDA MOHANDO CO.,LTD
Asaka Hanita
IKEDA MOHANDO CO.,LTD
Eri Oshima
Nagoya City University
Itsuki Nose
Nagoya City University
Yoko Inukai
Aichi Medical University School of Medicine
Makoto Tominaga
tominaga@nips.ac.jp

Nagoya City University

Article

Keywords: Crotamiton, Anoctamin 1 (ANO1), TMEM16A, Sweat, Transient Receptor Potential Vanilloid 4 (TRPV4)

Posted Date: November 12th, 2026

DOI: https://doi.org/10.21203/rs.3.rs-11201604/v1

License: This work is licensed under a Creative Commons Attribution 4.0 International License.
Read Full License

Additional Declarations: No competing interests reported.

Abstract

Sweating is essential for thermoregulation and skin homeostasis, and depends on coordinated neural signaling and ion transport in eccrine glands in humans. A central component of this process is the Ca^{2+}-activated chloride channel anoctamin 1 (ANO1), which mediates Cl^- efflux into the gland lumen following intracellular Ca^{2+} elevation, thereby driving osmotic fluid secretion. Transient receptor potential vanilloid 4 (TRPV4), a temperature-sensitive cation channel expressed in sweat gland acinar cells, contributes to this process by promoting Ca^{2+} influx and activating ANO1. In this study, we first found that *l*-menthol, which we previously reported to inhibit ANO1 and reduce sweating, inhibits TRPV4 activity, suggesting that blocking TRPV4 and ANO1 both of which were known to make a complex for exocrine function with water efflux is effective for inhibition of perspiration. Then we searched for the new compounds inhibiting both TRPV4 and ANO1, and focused on crotamiton, a topical antipruritic agent known to inhibit TRPV4. Using a whole-cell patch-clamp technique, we found that crotamiton inhibits ANO1-mediated currents. We also demonstrated that crotamiton suppresses sweating in both mice and humans while blocking of either TRPV4 or ANO1 alone was not sufficient for the significant inhibition of sweating in mice. These results indicate that compounds targeting both TRPV4 and ANO1 would be a promising strategy to develop effective antiperspirants.

Introduction

Perspiration is important function involved in the body temperature regulation. There are three types of sweating: thermoregulatory sweating, psychogenic sweating, and gustatory sweating [1, 2]. Among them, thermoregulatory sweating is the most important, and essential for adapting to the different ambient temperature. Excessive sweating is observed in some diseases such as primary focal hyperhidrosis or secondary hyperhidrosis such as hyperthyroidism, and it reduces quality of life (QOL) and leads to increased psychological burden and physical stress [3, 4]. Treatment of excessive sweating is routinely necessary in order to alleviate complications associated with various diseases and contribute to the mental and physical stability of patients.

The main active ingredients in antiperspirants currently used include aluminum salts (such as aluminum chlorohydrate and aluminum chloride hexahydrate). Aluminum salts react with sweat proteins to form gel plug in the sweat glands, thereby temporarily blocking the ducts of eccrine glands and inhibiting perspiration [5–8]. This treatment has been clinically validated and forms the core of current formulations. Additionally, antiperspirants are often combined with antimicrobials (isopropyl methylphenol), desiccants (silica), excipients and solvents, and skin-protective ingredients [6, 9–11]. In recent years, driven by health-conscious trends, there is growing demand for the development of new products that offer high safety and efficacy without relying on sweat gland occlusion [6, 9, 12, 13].

Sweating is triggered by the increase in sympathetic nerve activity when body senses a rise in ambient temperature [1, 14, 15]. In the clear cells of the secretory coil of eccrine glands, which account for the majority of human sweating, increase in intracellular Ca^{2+} concentrations triggered by cholinergic

stimulation opens Ca^{2+}-activated Cl^- channel acnoctamin1 (ANO1; also known as TMEM16A), allowing Cl^- secretion into the lumen [16–19] which drives water efflux through water channel, aquaporin 5 (AQP5), and various ions are secreted via other ion channels or transporters, resulting in sweating. In this mechanism, concentration gradients of Ca^{2+} and Cl^- ions play a crucial role [20, 21].

Generally, increase in intracellular Ca^{2+} concentrations in sweat glands is caused by Ca^{2+} ions released from ER downstream of muscarinic receptor type 3 activation by acetylcholine [18]. However, we recently reported that Ca^{2+} influx through TRPV4, a TRP channel with high Ca^{2+} permeability, also contribute to the activation of ANO1 through a physical complex with the two channels [22]. And the interaction between TRPV4 and ANO1 is now known to be broadly involved in the exocrine gland functions with water movement including saliva and tear secretion [23–26]. It should be noted that both TRPV4 and ANO1 is activated by warm temperature, which raises a concept that the TRPV4/ANO1 complex works locally by sensing ambient temperature [22]. In another word, sweating can be regulated by local temperature detection in addition to the control by sympathetic nervous system.

Thus, now we might develop a novel antiperspirant by focusing on the inhibition of complex of TRPV4/ANO1/AQP. Indeed, we observed that *l*-menthol, an ANO1 inhibitor, blocked acetylcholine-induced sweating in mouse food pad without involvement of TRPM8 [22]. This result prompted us to search for other known chemicals inhibiting TRPV4 and ANO1.

Results

l -menthol inhibits mouse and human TRPV4-mediated current responses

Ca^{2+} flowing in from TRPV4 activates ANO1, which alters water transport via Cl^- movement [23]. If the TRPV4/ANO1 complex is involved in sweating, inhibiting both TRPV4 and ANO1 channels would be more effective than inhibiting either channel alone. Because we observed before that *l*-menthol blocked ANO1-mediated currents *in vitro* and inhibited acetylcholine-induced sweating in mouse food pad [22, 25], we decided to examine whether *l* -menthol inhibits TRPV4, a partner of the ANO1 in the complex using a patch-clamp technique. We examined the effects of *l* -menthol on the TRPV4-mediated currents in the whole-cell configuration at -60 mV holding potential with applying ramp-pulses from − 100 to + 100 mV every 5 seconds in HEK293T cells. *l*-menthol (3 mM) rapidly inhibited human TRPV4 currents (Fig. 1A, B), which is consistent with the inhibition of GSK101-evoked intracellular Ca^{2+} increase by *l*-menthol in the mouse sweat gland acinar cells [22]. The inhibition did not show rapid recovery upon *l*-menthol washout. We also examined the effects of *l*-menthol in HEK293T cells expressing mouse TRPV4. Small outwardly rectifying currents, indicative of basal TRPV4 activation at 25 ^{o}C condition were inhibited by the treatment with *l*-menthol (3 mM). In the presence of *l*-menthol, we did not see significant activation of mouse TRPV4 by 50 nM GSK101, consistent with the irreversibility observed in human TRPV4 currents. Then, we observed significant TRPV4-mediated currents activated by GSK101 after 1 min washout of *l*-menthol which was gradually desensitized even in the presence of GSK101 (Fig. 1C, D). On the other hand, the GSK101-activated mouse TRPV4 currents were rapidly inhibited by 3 mM of *l*-menthol like in

the human TRPV4 currents, and partially recovered after long washout of *l*-menthol (Fig. 1E, F). In order to discriminate the *l*-menthol-induced inhibition of mouse TRPV4 currents from the desensitization, we compared the time from *l*-menthol application to 50% inhibition of the currents. The time necessary for 50% current inhibition was significantly shorter in the presence of *l*-menthol, clearly indicating the *l*-menthol-induced inhibition of mouse TRPV4 activity (Fig. 1G). In other words, the results suggest that menthol inhibits not only TRPV4 current but also ANO1 current in mice and human.

Crotamiton inhibits human ANO1

Above results suggest that compounds such as *l*-menthol, which inhibit both TRPV4 and ANO1, are effective in inhibiting perspiration. Indeed, it was reported that inhibition of ANO1 alone or TRPV4 alone was not efficient for inhibition of perspiration in humans [27–29]. Therefore, we looked for other chemicals inhibiting both TRPV4 and ANO1 as candidates for novel antiperspirants. We decided to focus on crotamiton which is widely used as an antipruritic agent through the inhibition of TRPV4 activation [30]. ANO1 channels exhibit weak outward rectification at low intracellular Ca^{2+} concentrations (200 nM), whereas the current-voltage relationship becomes linear at high intracellular Ca^{2+} concentrations (500 nM) (Supplementary Fig. 1A). We evaluated whether crotamiton inhibits ANO1 currents activated by intracellular 500 nM free Ca^{2+} using a whole-cell patch-clamp technique with a holding potential of 0 mV in HEK293T cells. Crotamiton reversibly inhibited ANO1-mediated currents, and the inhibited currents looked similar to the one at 0 intracellular Ca^{2+} (Supplementary Fig. 1A, Fig. 2A). This inhibitory effect was reversible, and the IC_{50} values were 1.28 ± 0.0015 mM (Fig. 2A-C). Crotamiton did not affect the current in HEK293T cells that do not express channel proteins (Supplementary Fig. 1B).

Crotamiton inhibits the acetylcholine-induced sweating in mice

Sweating occurs as water ions moves from the intracellular to the extracellular space along with the movement of Cl^- ions mediated by activated ANO1. Furthermore, since activation of TRPV4 also activates ANO1, we predicted that inhibition of both TRPV4 and ANO1 is essential for suppressing sweating. The fact that crotamiton inhibited both TRPV4- and ANO1-mediated current responses suggests that crotamiton may work as an antiperspirant. Then we evaluated whether crotamiton suppresses sweating in mouse food pads in the ambient temperature of 30 ^oC. After allowing the hind paws to dry for 30 minutes, sweating induced by the acetylcholine injection (100 μM, 5 minutes) to the hind paws was examined using the iodine-starch reaction to measure secreted amylase with or without topical application of 10% crotamiton [31]. In mice applied with crotamiton showed almost no sweat spots compared to untreated mice (Fig. 3A). This indicates that sweating was suppressed by the application of crotamiton in mice. On the other hand, it was reported that inhibiting TRPV4 or ANO1 alone did not suppress sweating in humans [27, 29]. Therefore, in the present study, we administered either HC-067047 (HC067), a TRPV4 inhibitor, or T16Ainh-A01 (A01), an ANO1 Cl^- channel inhibitor, to mice and compared their sweat-inhibiting effects using the iodine-starch reaction. The results showed that neither compound alone produced a significant sweat-inhibiting effect (Fig. 3B, C). However,

simultaneous application of both HC067 and A01 significantly suppressed sweating in the mice (Fig. 3D). These results suggest the importance of inhibiting both TRPV4 and ANO1, rather than either one alone, for the suppression of sweating.

Crotamiton inhibits thermogenic sweating in humans.

The above results suggest that crotamiton can work as an antiperspirant in human as well. Therefore, we tried to evaluate whether the topical application of crotamiton suppresses thermogenic sweating in human. We first examined the expression of TRPV4 and ANO1 in normal human sweat glands, and confirmed strong co-expression of the two proteins in the sweat gland acinar cells (Fig. 4). In the thermogenic sweating in human, the subjects were first randomly divided into the two groups; control and crotamiton. After acclimating the subjects for 50 minutes in an environment maintained at 23–24°C and 50% humidity, basal sweating was measured without any chemical application in the morning. Then, control solution (solvent for crotamiton preparation) or 10% crotamiton was applied to the same subjects in their upper arms and allowed to air dry for 10 minutes in the afternoon of the same day. Subjects were placed in an environment maintained at 40°C and 40% humidity, and sweat production was measured every 30 seconds for 10 minutes. Sweating rates in the 10% crotamiton-treated group were significantly lower than no application group (0.896 vs. 0.556 mg/cm²/10 min) (Fig. 5A). Sweating rates were similar between no application and control group in the morning session (0.567 vs. 0.557 mg/cm^2/10 min, respectively). And the anti-perspiration effects of crotamiton became evident just after starting crotamiton application in the cumulative analysis of the local sweating (Fig. 5B). This suggests that the application of 10% crotamiton suppresses sweating in human skin, similar to the plantar surface of mouse foot pads.

Discussion

Current antiperspirants primarily suppress sweating by physically occluding eccrine sweat ducts with aluminum salts. However, there is a growing need for alternative approaches that can effectively suppress sweating without relying on sweat gland occlusion. Sweating is regulated by a Ca^{2+}-dependent secretory mechanism in eccrine sweat glands, in which activation of ANO1 by intracellular Ca^{2+} promotes Cl^- secretion and subsequent water movement through AQP5. We recently found that Ca^{2+} influx through TRPV4 contributes to ANO1 activation through a physical interaction between TRPV4 and ANO1 in eccrine sweat glands. These findings raise the possibility that targeting the TRPV4-ANO1 pathway could provide a novel strategy for suppressing sweating without physically blocking sweat ducts. Therefore, we investigated whether pharmacological inhibition of TRPV4 and ANO1 can suppress sweat secretion and explored their potential as molecular targets for a novel antiperspirant strategy.

In this study, we clearly showed that *l*-menthol inhibits TRPV4-mediated currents (Fig. 1) and that crotamiton inhibits ANO1-mediated currents (Fig. 2). We also showed that crotamiton inhibits sweating in both mice and humans (Figs. 3 and 5), and co-expression of TRPV4 and ANO1 in human skin (Fig. 4). In the mouse experiments with A01 or HC067, the control group likely had fewer sweat spots than in the

experiments with crotamiton, possibly due to the difference in the used solvent. Together with our previous observation that *l*-menthol inhibited mouse ANO1 channel and sweating in mice and that crotamiton inhibits mouse TRPV4 [22, 30], we concluded that chemicals inhibiting both TRPV4 and ANO1 are effective to inhibit perspiration.

Humans sweat profusely in various conditions, such as autonomic dysfunction, menopausal symptoms, and hyperhidrosis [3, 32, 33]. Among these, hyperhidrosis is a condition characterized by abnormal sweating in localized areas, such as palms and soles, or throughout the body, regardless of temperature changes [34, 35]. Excessive sweating can interfere with daily and social activities and often leads to psychological stress. Aluminum chloride preparations and anticholinergic drugs are currently used to treat these conditions [12, 33, 36]. A TRPV4/ANO1/AQP5 complex, which mediates water secretion in sweat gland secretory cells, has been reported to be critical for exocrine function with water efflux including sweating [22–25]. Polydatin, which targets AQP5, has been reported to suppress sweating in mice and is attracting attention as a treatment for hyperhidrosis characterized by high AQP5 expression in humans [37–39]. On the other hand, drugs that target TRPV4 or ANO1 channels alone have not proven for their effectiveness in excessive sweating in the human clinical trials [17, 27–29, 40], suggesting that inhibition of TRPV4 or ANO1 alone is not sufficient to inhibit perspiration *in vivo*. In this study, we showed that crotamiton, which inhibits both TRPV4 and ANO1 channels, may serve as a new antiperspirant in humans. Since crotamiton has been used clinically for long time as an antipruritic agent and is proven for its safeness [41, 42]. And crotamiton concentration used in the human study (10%) is same as in the treatment as an antipruritic agent. In addition, the fact that *l*-menthol which also inhibits TRPV4 and ANO1 reduced perspiration in mice supports this logic [43–45]. Furthermore, screening for chemicals inhibiting both TRPV4 and ANO1 would be an effective strategy for the development of new antiperspirants.

Ca^{2+} influx through store-operated Ca^{2+} entry (SOCE) was reported to be involved in ANO1 activation and essential for sweating since perspiration was almost completely gone in the conditional KO mice in which either ORAI1 or STIM1 is deficient in skin keratinocytes [18, 46]. We are currently not sure that which mechanism is more predominantly working *in vivo*. Ca^{2+} influx through TRPV4 and ORAI1 could work in concert to activate ANO1. We are proposing that local temperature sensing through TRPV4 and ANO1 in skin keratinocytes is important for perspiration. In this regard, it should be noted that ORAI1, in conjunction with STIM1 is also known to act as a temperature-sensitive Ca^{2+} channel while STIM1/ORAI1-mediated Ca^{2+} influx is activated during the cooling phase after high heat exposure as a heat-off sensor. Based on this, we expect that TRPV4 could work as a Ca^{2+} influx pathway more effectively in the elevated ambient temperature condition. However, more detailed future studies would be needed to conclude this.

In conclusion, we raised a new concept that inhibition of the two proteins, TRPV4 and ANO1, is effective for blocking perspiration.

Materials and Methods

Cell Culture

Human embryonic kidney-derived 293T (HEK293T) (RIKEN BRC, Ibaraki, Japan) cells is cultured at 37 ^{o}C in humidified air containing 5% CO_2, in Dulbecco's modified Eagle's Medium (Wako, Osaka, Japan) containing 10% fetal bovine serum (Biowest SAS, Nuaillé, France), 100 units ml^{-1} penicillin (Invitrogen Corp.), 100 μg ml^{-1} streptomycin (Invitrogen Corp.), and 1% GlutaMAX (Invitrogen Corp.).

Transfection

For patch-clamp recordings, 1 μg mouse TRPV4 in pcDNA3 vector (cloned by RIKEN), 1 μg human TRPV4 in pcDNA3 vector (a generous gift from Dr. W. Liedtke), or 1 μg human ANO1 in pcDNA3.1 vector (a generous gift from Dr. L. Galietta), or 1 μg pcDNA3.1 vector (Invitrogen Corp.) and 0.1 μg pGreen Lantern 1 cDNA (Life Technologies) were transfected to HEK293T cells cultured in 35 mm dishes substituted with OPTI-MEM medium (Gibco Corp.) using Lipofectamine™ Transfection Reagent (Invitrogen Corp.) and Lipofectamine Plus Reagent (Invitrogen Corp.). After incubating for 3–4 h, the cells were reseeded on coverslips (MATSUNAMI GLASS IND., LTD, Osaka, Japan) and further incubated at 33°C for mouse and human TRPV4 to minimize the basal temperature-evoked activation or 37°C for human ANO1 in 5% CO_2. Patch-clamp recordings were performed 1 day after transfection.

Chemicals.

3 mM GSK1016790A (GSK101) is dissolved in dimethyl sulfoxide (DMSO) (Sigma-Aldrich; G0798). 2.5 M *l*-menthol is dissolved in ethanol (Sigma-Aldrich; 63670). Crotamiton is diluted from the original solution (Sigma-Aldrich; 128201) in ethanol. 100 mM HC-067047 (HC067) is dissolved in DMSO (Sigma-Aldrich; 326143). 10 mM TMEM16A Inhibitor, T16Ainh-A01 (A01) is dissolved in DMSO (Sigma Aldrich; 613551). 3.5% iodine is dissolved in ethanol (Sigma Aldrich; 326143). Acetylcholine chloride is dissolved in DMSO (Sigma-Aldrich; A6625). starch (Wako; 191–03985).

Electrophysiology

For whole-cell experiments of TRPV4, the bath solution: 140 mM NaCl, 5 mM KCl, 2 mM $MgCl_2$, 10 mM HEPES, and 10 mM glucose at pH 7.4 adjusted with NaOH; pipette solution: 140 mM KCl, 5 mM EGTA, and 10 mM HEPES at pH 7.4 adjusted with KOH. For whole-cell experiments of ANO1, the bath solution: 135 mM NMDG, 1 mM $MgCl_2$, 2 mM $CaCl_2$, 10 mM HEPES, and 10 mM glucose at pH 7.4 adjusted with HCl; pipette solution: 140 mM NMDG, 5 mM $MgCl_2$, 4.47 mM $CaCl_2$, 5 mM EGTA, and 10 mM HEPES at pH 7.4 adjusted with HCl. The free Ca^{2+} concentration of the pipette solution was maintained at 500 nM in most cases, and changed from 100 to 500 nM in some experiments calculated with the WEBMAXC STANDARD program (MaxChelator; Bers and Patton, University of California, Davis) [47]. Patch pipettes were made from borosilicate glass (type 8250, King Precision Glass) with a three-step protocol using a P-97 (Sutter Instrument). All experiments were performed at 25°C. The membrane potential was clamped at 0 mV for the ANO1 channel and at -60 mV for the TRPV4 channel. Series resistance and

membrane capacitance were compensated. Voltage-ramp pulses from − 100 to + 100 mV within 500 msec were applied every 5 sec. Data were sampled at 10 kHz and filtered at 5 kHz for whole-cell recording (Axopatch 200B Amplifier, Molecular Devices), and digitized with Digidata 1440A (Axon Instruments). Data were analyzed using pCLAMP 10.4 Software (Molecular Devices).

Animal.

Adult male and female C57Bl/6J mice (2–4 months of age, n = 8–11) were obtained from SLC. The animals were group housed under environmentally controlled conditions (temperature 24–26°C, relative humidity 40–60%) at a fixed 12-h light/dark cycle with food and water available ad libitum.

Iodine and starch test.

We conducted the experiment based on Nejsum's paper [31]. The reagents were prepared to the following concentrations immediately before the experiment: 10% crotamiton (diluted with 50% ethanol, 35% PBS and 5% DMSO), 10% starch (diluted with mineral oil (Wako Pure Chemical Industries), 100 mM acetylcholine chloride (diluted with saline), 1 mM A01 (diluted with ethanol), 1 mM HC067 (diluted with ethanol). For the 10% crotamiton control group, the solvent was used. For the other control groups, an amount of DMSO equal to the reagent was diluted with ethanol. Mice housed at 30 ^{o}C over 2 hours. The mice in the experiment were always placed on a heating pad. After 2% isoflurane (Wako Pure Chemical Industries) inhalation anesthesia, apply compounds to the hind foot paws using a brush. The solvent was applied to the right hind foot paw, and a reagent was applied to the left hind foot paw. After air-drying at room temperature for 30 minutes, 3.5% iodine/ethanol was applied with a brush to the hind foot paws and allowed to dry for 2 min. 10% starch solution dissolved in mineral oil was applied with a brush to the hind foot paws and allowed to dry. 100 μM Acetylcholine chloride (50 μL) was administered subcutaneously to the hind foot paws. Photographs of the hind foot paws were taken, and the number of spots was analyzed.

Ethics statement

All animal experiments were approved by the Institutional Animal Care and Use Committee of Nagoya City University (approval number: [24-016H03, 24-017H04, 24-018H04]) and were performed in accordance with the relevant institutional and national guidelines and regulations for the care and use of laboratory animals. The human study was approved by the Ethics Committee of (approval number: [C205]). The study was conducted in accordance with the Declaration of Helsinki and relevant institutional and national guidelines and regulations. Written informed consent was obtained from all participants prior to skin tissue collection. The mice used in the experiment were anesthetized with isoflurane and subsequently euthanized using the same agent.

Immunostaining for human samples

Immunofluorescence analysis was performed on formalin-fixed, paraffin-embedded skin tissue obtained from a patient with a melanocytic nevus and normal sweating. Tissue sections were cut at a thickness of

2–3 μm. This study was approved by the Ethics Committee of Kanazawa Medical University (C205), and all procedures were conducted in accordance with relevant guidelines and regulations. After deparaffinization and antigen retrieval, primary and secondary antibodies were applied sequentially, followed by nuclear counterstaining. Fluorescence signals were examined using a fluorescence microscope (Zeiss). After fluorescence imaging, the same tissue section was stained with hematoxylin and eosin (H&E) to confirm the identity and morphology of the corresponding eccrine sweat gland. As primary antibodies, we used an anti-TRPV4 antibody (guinea pig polyclonal) (made by Dr. Mizuho Kido in Saga University) at a 1:1,000 dilution [48] and an anti-ANO1 antibody (ab53213) at a 1:100 dilution. As secondary antibodies, we used Alexa Fluor 488 donkey anti-guinea pig IgG antibody (A17655) at a 500-fold dilution and Alexa Fluor 594 goat anti-rabbit IgG antibody (AB_2338059) at a 200-fold dilution.

Measurement of human sweat rate

The study involving human subjects was reviewed and approved by the institutional ethics committee (Safety Evaluation Committee) of IKEDA MOHANDO CO., LTD. Written informed consent was obtained from all participants prior to the study. We confirmed that all experiments were conducted in accordance with the relevant guidelines and regulations.

Measurements were taken twice a day at the same sites on the forearm. Subjects acclimated for 1 hour at 23–24 ^{o}C, 50%, then moved to 40 ^{o}C, 40% where sweat production was measured every 30 seconds for 10 minutes. Vehicle (composed of 50% water and 50% ethanol) or 10% crotamiton (composed of 10% crotamiton, 40% water and 50% ethanol) was applied 50 μL at 50 minutes after acclimation began. The sweat volume measured every second over time using flow-compensated ventilation capsule type sweat meter SMN-1000 (SKINOS Co., Ltd.) was analyzed as local sweat rate every 30 seconds.

The total sweat volume (AUC_{total}) for each subject was calculated according to the following formula.

$$AUC_{total} = \int_{0}^{600\mathrm{sec}} \{ \mathrm{v}(\mathrm{t}) - \mathrm{v}(\mathrm{base}) \}\, dt \ \text{[mg/cm2]}$$

Statistical analyses.

Statistical analyses were performed with Origin Pro 2026 J (OriginLab, United States). The Mann–Whitney U test was used to determine the 50% inhibition time. Iodine and starch test were analyzed with the Wilcoxon signed-rank test or unpaired t-test. Two-way repeated-measures ANOVA, followed by Šídák's multiple-comparisons test was performed for Inhibition of thermal sweating in human. Values of $p < 0.05$ were accepted as statistically significant differences.

Declarations

Competing interests

The authors declare no competing interests.

Author Contribution

M.I. conducted all experiments except measurement of human sweat volume and staining of human sweat gland cells. K.K. A.H. and H.K. performed measurement of human sweat volume. Y.I. joined the discussion about the human study. K.S. carried out a staining experiment on human sweat gland cells. M.T. designed the experiments. M.I. and M.T. wrote the manuscript and prepared the figures with input from the other authors. M.T. supervised the project. E.O. and I.N. contributed to data interpretation and discussion. All authors have read and approved the final manuscript.

Acknowledgements

We thank Mizuho Kido for providing anti-TRPV4 antibody. This work was supported by Grant-in-Aid for Outstanding Research Group Support Program in Nagoya City University Grant Number 2401101 and grants to MT from a Grant-in-Aid for Scientific Research from the Ministry of Education, Culture, Sports, Science and Technology in Japan (#21H02667 and #23H04943).

Data Availability

All data generated or analyzed during this study are included in this published article and its supplementary information files.

References

1. Shibasaki, M. & Crandall, C. G. Mechanisms and controllers of eccrine sweating in humans. *Front. Biosci. (Schol Ed)*. **2**, 685–696. 10.2741/s94 (2010).
2. Lee, T. S. Physiological gustatory sweating in a warm climate. *J. Physiol.* **124**, 528–542. 10.1113/jphysiol.1954.sp005126 (1954).
3. Wohlrab, J., Bechara, F. G., Schick, C., Naumann, M. & Hyperhidrosis A Central Nervous Dysfunction of Sweat Secretion. *Dermatol. Ther. (Heidelb)*. **13**, 453–463. 10.1007/s13555-022-00885-w (2023).
4. Parashar, K., Adlam, T. & Potts, G. The Impact of Hyperhidrosis on Quality of Life: A Review of the Literature. *Am. J. Clin. Dermatol.* **24**, 187–198. 10.1007/s40257-022-00743-7 (2023).
5. Sakhawoth, Y. et al. Real time observation of the interaction between aluminium salts and sweat under microfluidic conditions. *Sci. Rep.* **11**, 6376. 10.1038/s41598-021-85691-8 (2021).
6. Teerasumran, P., Velliou, E., Bai, S. & Cai, Q. Deodorants and antiperspirants: New trends in their active agents and testing methods. *Int. J. Cosmet. Sci.* **45**, 426–443. 10.1111/ics.12852 (2023).

7. Bretagne, A. et al. The mechanism of eccrine sweat pore plugging by aluminium salts using microfluidics combined with small angle X-ray scattering. *Soft Matter*. **13**, 3812–3821. 10.1039/c6sm02510b (2017).
8. Shelley, W. B. & Hurley, H. J. Jr. Studies on topical antiperspirant control of axillary hyperhidrosis. *Acta Derm Venereol.* **55**, 241–260. 10.2340/0001555555241260 (1975).
9. Oliveira, E. C. V. et al. Deodorants and antiperspirants: identification of new strategies and perspectives to prevent and control malodor and sweat of the body. *Int. J. Dermatol.* **60**, 613–619. 10.1111/ijd.15418 (2021).
10. Naseef, P. P. et al. Design and development of antiperspirant formulation from natural extract: An overview. *Int. J. Pharm. Chem. Anal.* **11**, 108–111. 10.18231/j.ijpca.2024.015 (2024).
11. Zirwas, M. D. & Moennich, J. Antiperspirant and deodorant allergy: diagnosis and management. *J. Clin. Aesthetic Dermatology*. **1**, 38–43 (2008).
12. McConaghy, J. R. & Fosselman, D. Hyperhidrosis: Management Options. *Am. Family Phys.* **97**, 729–734 (2018).
13. Scholes, K. T., Crow, K. D., Ellis, J. P., Harman, R. R. & Saihan, E. M. Axillary hyperhidrosis treated with alcoholic solution of aluminium chloride hexahydrate. *Br. Med. J.* **2**, 84–85. 10.1136/bmj.2.6130.84 (1978).
14. Hu, Y., Converse, C., Lyons, M. C. & Hsu, W. H. Neural control of sweat secretion: a review. *Br. J. Dermatol.* **178**, 1246–1256. 10.1111/bjd.15808 (2018).
15. Cramer, M. N., Gagnon, D., Laitano, O. & Crandall, C. G. Human temperature regulation under heat stress in health, disease, and injury. *Physiol. Rev.* **102**, 1907–1989. 10.1152/physrev.00047.2021 (2022).
16. Baker, L. B. Physiology of sweat gland function: The roles of sweating and sweat composition in human health. *Temp. (Austin)*. **6**, 211–259. 10.1080/23328940.2019.1632145 (2019).
17. Ertongur-Fauth, T., Hochheimer, A., Buescher, J. M., Rapprich, S. & Krohn, M. A novel TMEM16A splice variant lacking the dimerization domain contributes to calcium-activated chloride secretion in human sweat gland epithelial cells. *Exp. Dermatol.* **23**, 825–831. 10.1111/exd.12543 (2014).
18. Concepcion, A. R. et al. Store-operated Ca2 + entry regulates Ca2+-activated chloride channels and eccrine sweat gland function. *J. Clin. Invest.* **126**, 4303–4318. 10.1172/JCI89056 (2016).
19. Baker, L. B. & Wolfe, A. S. Physiological mechanisms determining eccrine sweat composition. *Eur. J. Appl. Physiol.* **120**, 719–752. 10.1007/s00421-020-04323-7 (2020).
20. Patel, R., Heard, K., Chen, L., Bollag, W. B. & X. & Aquaporins in the Skin. *Adv. Exp. Med. Biol.* **969**, 173–191. 10.1007/978-94-024-1057-0_11 (2017).
21. Song, Y., Sonawane, N. & Verkman, A. S. Localization of aquaporin-5 in sweat glands and functional analysis using knockout mice. *J. Physiol.* **541**, 561–568. 10.1113/jphysiol.2001.020180 (2002).
22. Kashio, M. et al. Involvement of TRPV4 in temperature-dependent perspiration in mice. *Elife* **13** 10.7554/eLife.92993 (2024).

23. Takayama, Y., Shibasaki, K., Suzuki, Y., Yamanaka, A. & Tominaga, M. Modulation of water efflux through functional interaction between TRPV4 and TMEM16A/anoctamin 1. *FASEB J.* **28**, 2238–2248. 10.1096/fj.13-243436 (2014).
24. Derouiche, S., Takayama, Y., Murakami, M. & Tominaga, M. TRPV4 heats up ANO1-dependent exocrine gland fluid secretion. *FASEB J.* **32**, 1841–1854. 10.1096/fj.201700954R (2018).
25. Takayama, Y., Furue, H. & Tominaga, M. 4-isopropylcyclohexanol has potential analgesic effects through the inhibition of anoctamin 1, TRPV1 and TRPA1 channel activities. *Sci. Rep.* **7**, 43132. 10.1038/srep43132 (2017).
26. Takayama, Y. & Tominaga, M. Interaction between TRP channels and anoctamins. *Cell. Calcium*. **121**, 102912. 10.1016/j.ceca.2024.102912 (2024).
27. Fujii, N. et al. TMEM16A blockers T16Ainh-A01 and benzbromarone do not modulate the regulation of sweating and cutaneous vasodilatation in humans in vivo. *Exp. Physiol.* **107**, 844–853. 10.1113/EP090521 (2022).
28. Fujii, N. et al. Evidence for TRPV4 channel induced skin vasodilatation through NOS, COX, and KCa channel mechanisms with no effect on sweat rate in humans. *Eur. J. Pharmacol.* **858**, 172462. 10.1016/j.ejphar.2019.172462 (2019).
29. Fujii, N. et al. TRPV4 channel blockade does not modulate skin vasodilation and sweating during hyperthermia or cutaneous postocclusive reactive and thermal hyperemia. *Am. J. Physiol. Regul. Integr. Comp. Physiol.* **320**, R563–R573. 10.1152/ajpregu.00123.2020 (2021).
30. Kittaka, H., Yamanoi, Y. & Tominaga, M. Transient receptor potential vanilloid 4 (TRPV4) channel as a target of crotamiton and its bimodal effects. *Pflugers Arch.* **469**, 1313–1323. 10.1007/s00424-017-1998-7 (2017).
31. Nejsum, L. N. et al. Functional requirement of aquaporin-5 in plasma membranes of sweat glands. *Proc. Natl. Acad. Sci. U S A*. **99**, 511–516. 10.1073/pnas.012588099 (2002).
32. Coon, E. A. & Cheshire, W. P. Jr. Sweating Disorders. *Continuum (Minneap Minn)*. **26**, 116–137. 10.1212/CON.0000000000000813 (2020).
33. Haider, A. & Solish, N. Focal hyperhidrosis: diagnosis and management. *CMAJ* 172, 69–75, (2005). 10.1503/cmaj.1040708
34. Nawrocki, S. & Cha, J. The etiology, diagnosis, and management of hyperhidrosis: A comprehensive review: Therapeutic options. *J. Am. Acad. Dermatol.* **81**, 669–680. 10.1016/j.jaad.2018.11.066 (2019).
35. Stuart, M. E., Strite, S. A. & Gillard, K. K. A systematic evidence-based review of treatments for primary hyperhidrosis. *J. Drug Assess.* **10**, 35–50. 10.1080/21556660.2020.1857149 (2020).
36. Hornberger, J. et al. Recognition, diagnosis, and treatment of primary focal hyperhidrosis. *J. Am. Acad. Dermatol.* **51**, 274–286. 10.1016/j.jaad.2003.12.029 (2004).
37. Du, Q., Lin, M., Yang, J. H., Chen, J. F. & Tu, Y. R. Overexpression of AQP5 Was Detected in Axillary Sweat Glands of Primary Focal Hyperhidrosis Patients. *Dermatology* **232**, 150–155. 10.1159/000444081 (2016).

38. Chen, J. F. et al. Polydatin ameliorates hyperhidrosis by targeting Aqp5 in a mouse model. *Front. Pharmacol.* **16**, 1589143. 10.3389/fphar.2025.1589143 (2025).
39. Iizuka, T., Suzuki, T., Nakano, K. & Sueki, H. Immunolocalization of aquaporin-5 in normal human skin and hypohidrotic skin diseases. *J. Dermatol.* **39**, 344–349. 10.1111/j.1346-8138.2011.01327.x (2012).
40. Oh, U. & Jung, J. Cellular functions of TMEM16/anoctamin. *Pflugers Arch.* **468**, 443–453. 10.1007/s00424-016-1790-0 (2016).
41. Burckhardt, W. R. R. Experience with the New Anti-Scabies Remedy Eurax (Geigy). *Schweizerische Medizinische Wochenschrift*. **76** (47), 1213–1214 (1946).
42. Couperus, M. The use of N-ethyl-o-crotonotoluidide in the treatment of scabies and various pruritic dermatoses. *J. Invest. Dermatol.* **13**, 35–42. 10.1038/jid.1949.63 (1949).
43. Smith, E. B., King, C. A. & Baker, M. D. Crotamiton lotion in pruritus. *Int. J. Dermatol.* **23**, 684–685. 10.1111/j.1365-4362.1984.tb01235.x (1984).
44. Sekine, R., Satoh, T., Takaoka, A., Saeki, K. & Yokozeki, H. Anti pruritic effects of topical crotamiton, capsaicin, and a corticosteroid on pruritogen-induced scratching behavior. *Exp. Dermatol.* **21**, 201–204. 10.1111/j.1600-0625.2011.01433.x (2012).
45. Karacic, I. & Yawalkar, S. J. A single application of crotamiton lotion in the treatment of patients with pediculosis capitis. *Int. J. Dermatol.* **21**, 611–613. 10.1111/j.1365-4362.1982.tb02048.x (1982).
46. Concepcion, A. R. & Feske, S. Regulation of epithelial ion transport in exocrine glands by store-operated Ca(2+) entry. *Cell. Calcium*. **63**, 53–59. 10.1016/j.ceca.2016.12.004 (2017).
47. Bers, D. M., Patton, C. W. & Nuccitelli, R. A practical guide to the preparation of Ca(2+) buffers. *Methods Cell. Biol.* **99**, 1–26. 10.1016/B978-0-12-374841-6.00001-3 (2010).
48. Kitsuki, T. et al. Enhanced junctional epithelial permeability in TRPV4-deficient mice. *J. Periodontal Res.* **55**, 51–60. 10.1111/jre.12685 (2020).

Figures

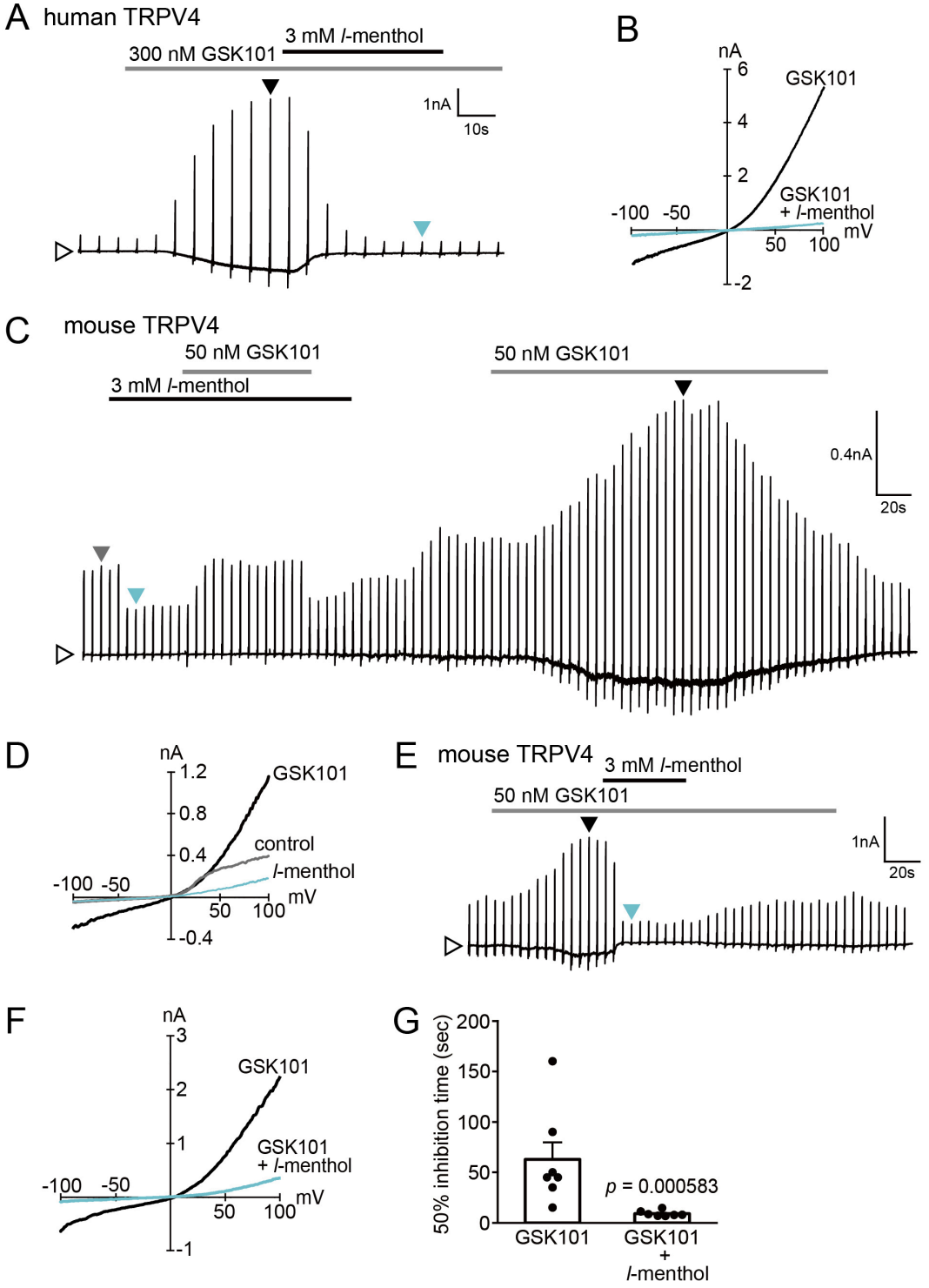


Figure 1

Mouse and human TRPV4 inhibition by *l*-menthol in whole-cell patch-clamp recordings.

A. A representative trace of GSK1016790A (GSK101)-induced human TRPV4 current held at -60 mV and its inhibition by *l*-menthol. (3 mM). Voltage ramp-pulses (-100 to +100 mV for 500 msec) were applied every 5 seconds. **B.** Current-voltage (I-V) relationships of GSK101-induced currents with and without *l*-

menthol from the trace shown in **A** (arrow heads). **C.** A representative trace of the GSK1016790A (GSK101)-induced mouse TRPV4 current held at -60 mV and its inhibition by *l*-menthol. **D.** I-Vrelationships of basal and GSK101-induced currents from the trace shown in **C** (arrow heads). **E.** A representative trace of the GSK101-induced mouse TRPV4 current inhibited by *l*-menthol. **F.** I-V relationships of the GSK101-induced currents before and after *l*-menthol application from the trace shown in **E** (arrow heads). **G.** Comparison of the time (sec) needed for 50 % inhibition of the GSK101-induced mouse TRPV4 currents with or without *l*-menthol. n = 7. White arrowheads: 0 current levels. Mean ± S.E.M.

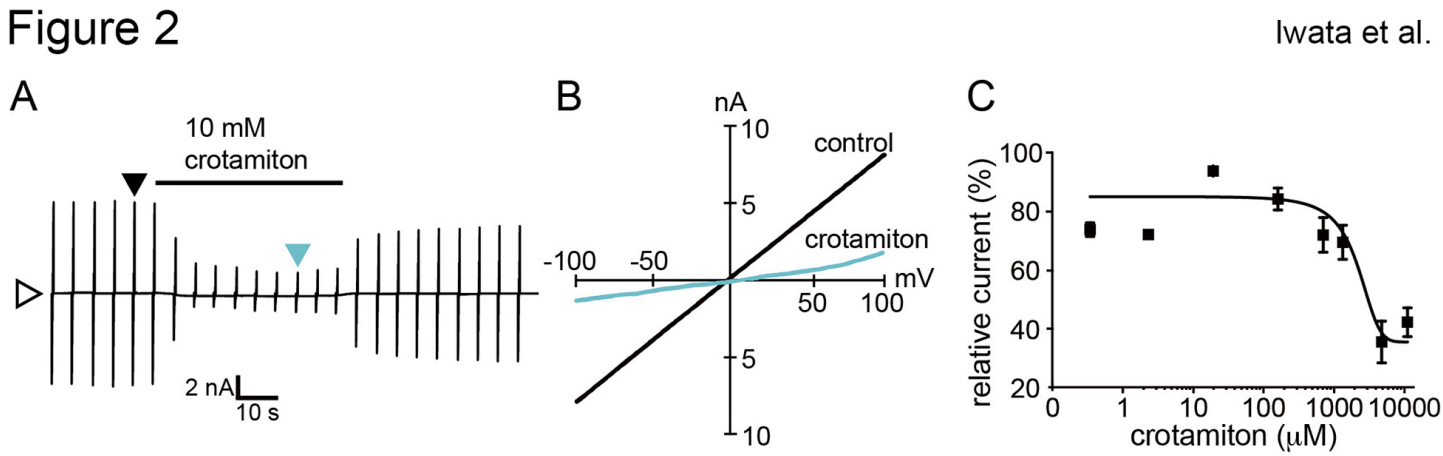


Figure 2

Human ANO1 inhibition by crotamiton treatment in whole-cell patch-clamp recordings.

A. A representative trace of intracellular Ca^{2+} (500 nM)-induced hANO1 currents held at 0 mV and its inhibition by crotamiton (10 mM). Voltage ramp-pulses (-100 to +100 mV for 500 msec) were applied every 5 seconds. **B.** I-V relationships of hANO1 currents before and after application of crotamiton shown in **A** (arrow heads). **C.** A dose-dependent curve for crotamiton-induced inhibition of hANO1 currents at +100 mV. Means ± SEM. n = 3, 2, 4, 6, 6, 11, 7, 9 and 5 for 0.1, 1, 10, 100, 500, 1000, 4000, and 10000 mM crotamiton, respectively. The IC_{50} was 1.28 ± 0.00145 mM. A white arrowhead: 0 current level.

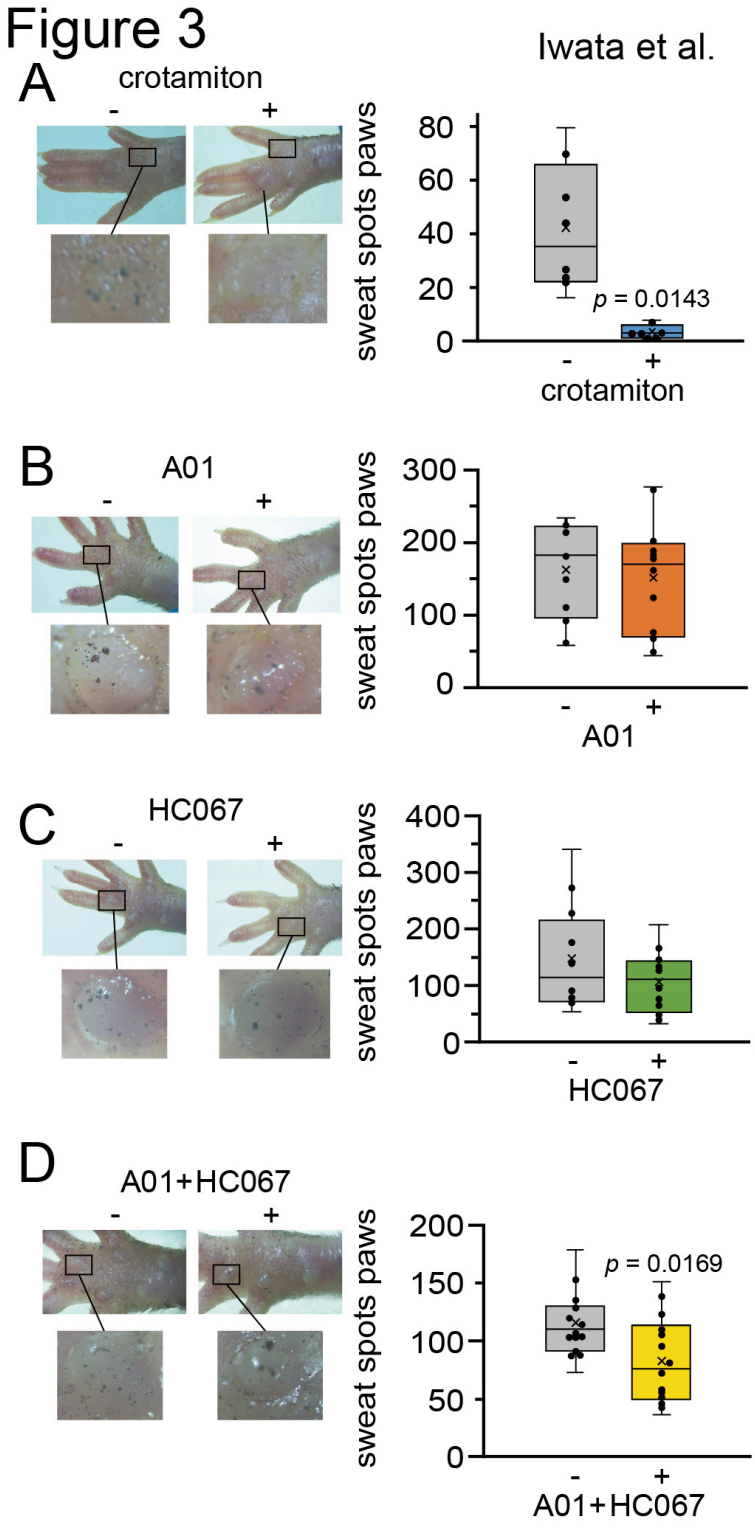


Figure 3

Inhibition of the stimulated sweating in mouse hind paws following topical application of several chemicals.

A-D. Representative stimulated sweat spots formed in hind paws of wild-type mice 5 minutes after acetylcholine (100 mM) injection following application of crotamiton (**A**), T16Ainh-A01 (A01, **B**), HC-

067047 (HC067, **C**) or A01+HC067 (**D**) (left). Comparison of sweat spots/paw without and with treatment of crotamiton (**A**), A01 (**B**), HC067 (**C**) or A01+HC067 (**D**); n = 8 mice (**A**), n = 12 mice (**B, C**), n = 14 mice (**D**) (right). Horizontal lines inside the boxes indicate the median, and 'x' marks indicate the mean. Each plot represents the value of a sample within the box-and-whisker plot.

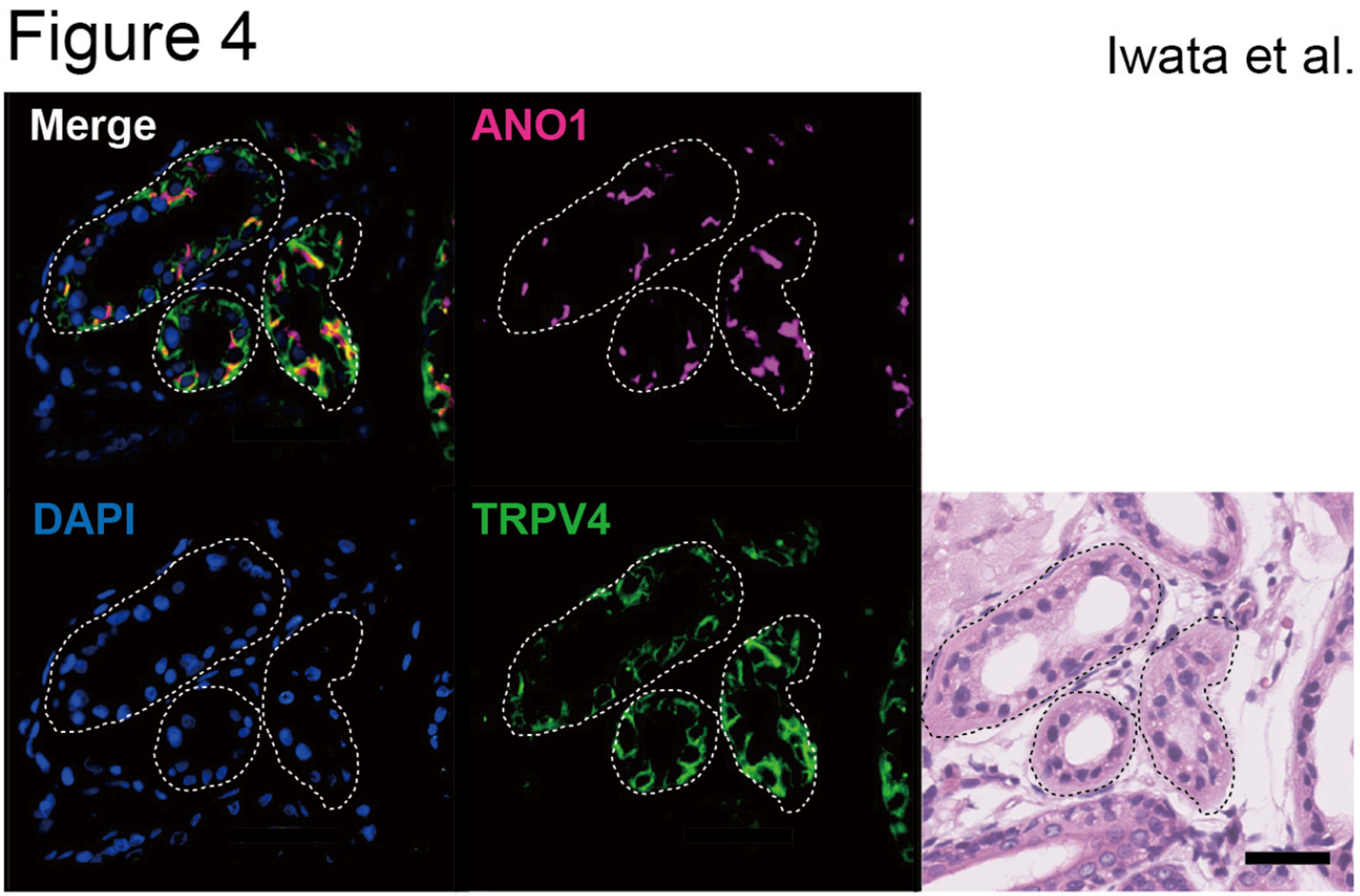


Figure 4

Co-expression of TRPV4 and ANO1 in human sweat glands.

Representative ANO1 and TRPV4 staining in sweat glands from normohidrotic human skin. magenta: ANO1, green: TRPV4, blue: DAPI (nuclei). Scale bar: 40 μm.

Figure 5

Iwata et al.

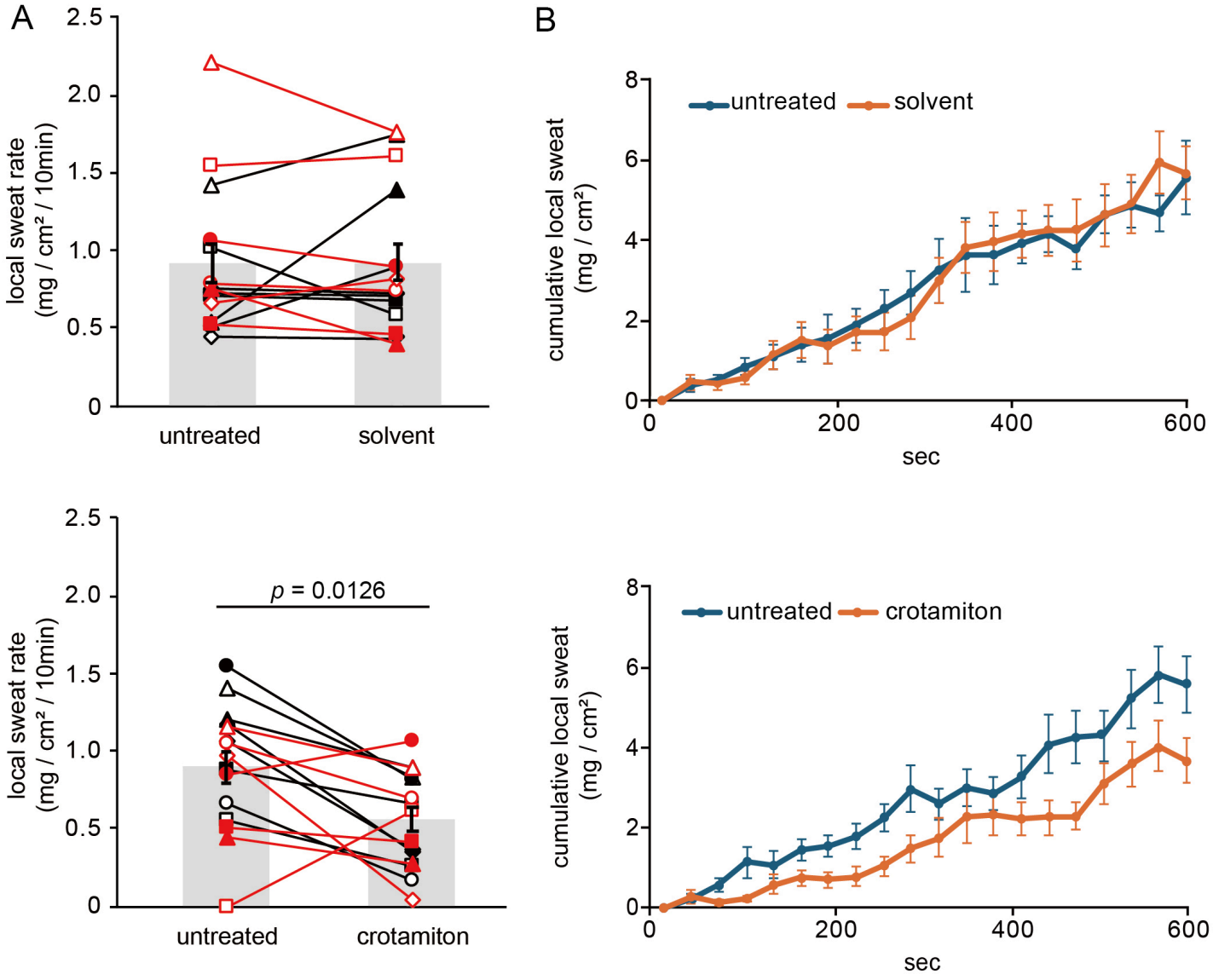


Figure 5

Inhibition of thermal sweating by 10 % crotamiton in human.

A. Local sweat rates (mg / cm^2 / 10 min). [up] untreated (AM) and treated with solvent (PM). [down] untreated (AM) and treated with 10 % crotamiton (PM). **B.** Cumulative local sweat (mg / cm^2) for 10 min. [up] untreated (AM) and treated with solvent (PM). [down] untreated (AM) and treated with 10 % crotamiton (PM). Black plots: male, red plots: female. n = 15.

Supplementary Files

This is a list of supplementary files associated with this preprint. Click to download.

- Iwataetal.revisedSupp.Figure1.pdf
- Iwataetal.Suppl.data.pdf